



Short communication

6-Cyclohexylmethoxy-5-(cyano-*NNO*-azoxy)pyrimidine-4-amine: A new scaffold endowed with potent CDK2 inhibitory activity



Donatella Boschi^a, Paolo Tosco^a, Naveen Chandra^a, Shilpi Chaurasia^a, Roberta Fruttero^{a,*}, Roger Griffin^b, Lan-Zhen Wang^b, Alberto Gasco^a

^a Dipartimento di Scienza e Tecnologia del Farmaco, Università degli Studi di Torino, via Pietro Giuria 9, 10125 Torino, Italy

^b Newcastle Cancer Centre, Northern Institute for Cancer Research and School of Chemistry, Newcastle University, Newcastle upon Tyne, UK

ARTICLE INFO

Article history:

Received 23 March 2013

Received in revised form

6 June 2013

Accepted 17 July 2013

Available online 11 August 2013

Keywords:

CDK inhibitor

CDK2 selective inhibitor

Cyano-*NNO*-azoxy

5-Substituted pyrimidine-4-amine

Water-mediated hydrogen bond

ABSTRACT

Substitution of the cyano-*NNO*-azoxy moiety (NC–N=(O)N–) for the nitroso group in NU6027, a potent and selective CDK2 inhibitor, affords a compound with slightly improved potency and comparable selectivity profile. A molecular modelling study indicates for this new scaffold a binding mode similar to the one adopted by other purine and pyrimidine analogues, and suggests a relevant role for a conserved water molecule in stabilizing the bioactive pose of this and other pyrimidine ligands. The introduction of aminosulfonylphenyl substituents on the 2-amino group of the pyrimidine increased the CDK2 inhibitory potency by two orders of magnitude, while maintaining the same degree of selectivity.

© 2013 Elsevier Masson SAS. All rights reserved.

1. Introduction

The division of eukaryotic cells occurs in four phases (G_1 , S , G_2 , M) and cell-cycle progression is regulated by several members of a family of cyclin-dependent serine/threonine kinases (CDKs). To date, eleven members of this family have been identified, respectively named CDK1 (also known as *cdc2*), and CDK2–CDK11 [1,2]. The activity of these kinases is dependent on their cyclin partners. The principal CDK/cyclin pairs involved in regulating cell division are CDK1/cyclinB, CDK2/cyclinA, CDK2/cyclinE, and CDK4,6/cyclins of the D family. The inhibition of CDKs by small molecules continues to attract considerable attention as a strategy to exploit in developing anticancer drugs [3–5]. A variety of these inhibitors have been described, some of which are currently under clinical evaluation [4]; an oral selective inhibitor for CDK 4 and 6, palbociclib [6], has recently received Breakthrough Therapy designation by the FDA for potential treatment of patients with breast cancer. The chemotype exemplified by **1** (6-(cyclohexylmethoxy)-5-

nitrosopyrimidine-2,4-diamine, NU6027; Fig. 1) has been developed as a potent and selective CDK2 inhibitor. In this structure, the presence of an intramolecular hydrogen bond between the adjacent 5-nitroso and 4-amino groups forces the molecule to assume a pseudo-purine geometry, which is reminiscent of the purine scaffold **2** (6-(cyclohexylmethoxy)-9*H*-purine-2-amine, NU2058; Fig. 1), another selective CDK2 inhibitor [7]. X-ray analysis of the CDK2/NU2058 and CDK2/NU6027 crystal complexes shows that the two products establish the same key interactions with the backbone of amino acid residues within the ATP-binding site of CDK2, namely a triplet of H-bonds (2-NH₂ to Leu83, N3 to Leu83, N9–H to Glu81, and 2-NH₂ to Leu83, N1 to Leu83, 4-NH₂ to Glu81, respectively) [7]. Structure–activity relationships (SAR) have been studied in detail for these two leads [8–10]. In particular, it has been observed that a *p*-aminosulfonylphenyl substituent on the 2-NH₂ group (e.g. **3**, NU6102; Fig. 1) confers high inhibitory potency, due to additional hydrophobic and hydrogen bonding interactions within the binding pocket. Extensive structural modification of scaffold **1** has confirmed the crucial role of the nitroso group at the 5-position of the pyrimidine; only nitro, formyl, and acetyl moieties are tolerated as possible alternatives at this position [10]. In this paper, we show how a potent and quite selective CDK2 inhibitor can be obtained by replacing the NO group in **1** with a cyano-*NNO*-azoxy moiety (NC–N(O)=N–, compound **5**; Fig. 1). This function was

* Corresponding author. Tel.: +39 (0)116707850; fax: +39 (0)116707286.

E-mail address: roberta.fruttero@unito.it (R. Fruttero).

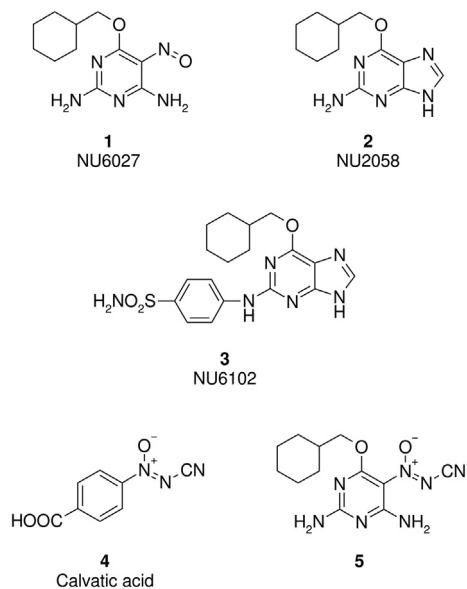


Fig. 1. Structures of compounds 1–5.

discovered while studying an antibiotic isolated from three different sources, *Calvatia lilacina*, *Calvatia craniformis* and *Lycoperdon pyriforme*; the antibiotic was assigned the 4-[(*Z*)-cyano-*NNO*-azoxy]benzoic acid structure **4** [11–13]. The synthesis, and the structural and biological characterization of some lead compounds based on this new scaffold are reported below. Structure–activity relationships are also discussed, and a binding mode hypothesis based on a molecular modelling study is proposed.

2. Chemistry

The preparation of the final products **5**, **6**, and **9** is outlined in Fig. 2. The scaffold **5** was easily obtained using a method described elsewhere [14]. This procedure involves treating the 5-nitroso derivative **1** with (diacetoxyiodo)benzene (IBA) and cyanamide (NH_2CN) in dry CH_3CN . The action of HCl on **5**, dissolved in a THF/ H_2O mixture, afforded the related amide **6**. The best yields in the preparation of the final (4-methylphenyl)sulfonyl derivative **9** were obtained by protecting the two amino groups in **1** as acetyl derivatives. When the reaction was carried out starting directly from **1**, compound **7** was obtained. It is known that derivatives of the [1,2,5]oxadiazolo-[3,4-*d*]pyrimidine scaffold, such as compound **7**, can be prepared in anhydrous DMF by action of a slight excess of IBA on the related 5-nitrosopyrimidine-4-amines, in the presence of LiH [15]. Conversely, a mixture of derivatives **8** and **7a** was obtained by treating the diacetylated intermediate **1a** with (4-methylphenyl)sulfonamide (TsNH_2) and IBA dissolved in $\text{CH}_2\text{Cl}_2/\text{CH}_3\text{CN}$.

Deprotection of the amino groups in **8**, carried out with ZnCl_2 in ethanol, yielded the desired final product **9**. The preparation of final derivatives **14** and **16**, bearing substituted (aminosulfonyl) phenyl moieties at the N2 position, is outlined in Fig. 3. A mixture of *n*-butylsulfonylpyrimidine **10** and 4-amino-*N*-methylbenzenesulfonamide **11** dissolved in 2,2,2-trifluoroethanol (TFE) was treated with trifluoroacetic acid (TFA) to afford **12**. Nitrosation of the latter yielded the related 5-nitroso-substituted compound **13**, which in turn, upon treatment under the same conditions used to prepare **5** from **1**, yielded the expected product **14**. Compound **16** was obtained following the same procedure,

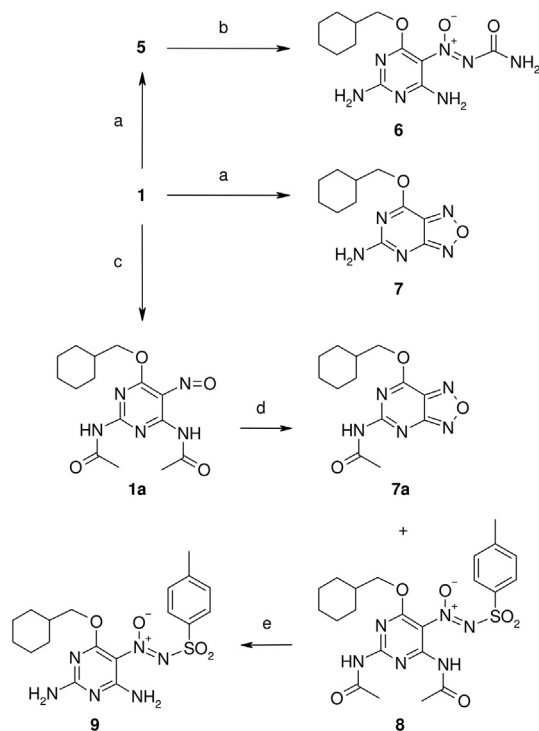


Fig. 2. Synthetic pathway leading to final products **5**, **6** and **9**. Reagents and conditions: a) NH_2CN , IBA, dry CH_3CN ; b) HCl gas, THF/ H_2O , 0 °C; c) Ac_2O , 50 °C; d) TsNH_2 , IBA, dry $\text{CH}_2\text{Cl}_2/\text{CH}_3\text{CN}$ 2/1, 40 °C; e) ZnCl_2 , EtOH, 65 °C.

starting from **15**. For the purpose of the present study, the ^1H NMR resonances of the 4-amino groups in compounds **1**, **5**, **6**, **9**, **14** and **16** deserve some comments. The signal of the 4- NH_2 group in derivative **1**, recorded in $\text{DMSO}-d_6$ at room temperature, is split into two neat signals, which fall at 10.09 and 8.01 ppm, respectively. The unusually low-field signal at 10.09 ppm can be assigned to the N–H proton chelated by the NO group [16]: the two protons experience quite different local magnetic fields, as a consequence of the strong anisotropic effect exerted by the nitroso function.

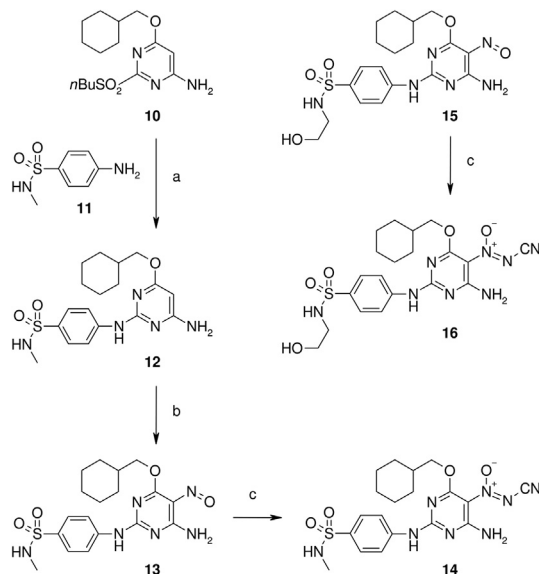


Fig. 3. Synthesis of compounds **14** and **16**. Reagents and conditions: a) **11**, TFA/TFE, reflux; b) NaNO_2 , $\text{AcOH}/\text{H}_2\text{O}$, 100 °C; c) NH_2CN , IBA, dry CH_3CN .

Table 1
Inhibitory activity of compounds **1**, **5**, **6**, **9**, **14**, **16** against different CDK isoforms.

CDK isoform	IC ₅₀ (μM) ^a					
	1	5	6	9	14	16
CDK2/A	2.2 ± 0.6 ^b	0.94	53.3	48% ^c	0.0039	0.0025
CDK1/B	2.9 ± 0.1 ^b	– ^d	– ^d	– ^d	0.14	0.071
CDK4/D	24% ^e	– ^d	– ^d	– ^d	1.05	0.99
CDK7/H	26% ^e	– ^d	– ^d	– ^d	1.5	1.55
CDK9/T	36% ^e	– ^d	– ^d	– ^d	1.66	0.875
CDK5/P25	– ^d	– ^d	– ^d	– ^d	0.775	0.56

^a CDK-inhibition was determined in duplicate at a minimum of five different inhibitor concentrations.

^b Ref. [17].

^c Percent inhibition at 100 μM.

^d Not tested.

^e Percent inhibition at 10 μM.

Conversely, in models **5**, **6**, **9**, **14** and **16** the 4-NH₂ signals appear as a broadened singlet.

3. Results and discussion

The pyrimidine derivatives were evaluated for CDK inhibitory activity using published procedures [17]. The results are shown in Table 1, together with the inhibitory potencies of compound **1**, taken as reference. Analysis of the data shows that the new scaffold **5** displays an inhibitory potency on the CDK2 isoform that is about twice that of reference **1**. The substitution of the cyano group on the azoxy function with different electron-withdrawing moieties, such as the amide and phenylsulfonyl groups (products **6** and **9**, respectively), induces a marked decrease in the inhibitory potency in both cases; this is more pronounced in **9**, probably as a consequence of the excessive steric bulk of the phenylsulfonyl moiety. Compounds **14** and **16** were designed based on the knowledge that the introduction of RNHSO₂C₆H₅– groups on the 2-NH₂ group of **1** affords very potent and selective CDK2 inhibitors, as discussed above. Indeed, the same trend is observed when this structural manipulation is carried out on scaffold **5**: products **14** and **16** are, respectively, about 240- and 400-fold more potent than the lead. Moreover, they are highly selective for CDK2, being some thirty times more potent compared with CDK1 and over two orders of magnitude with respect to the other isoforms. The same compounds were evaluated for growth inhibitory activity on three different cell lines, namely A2780 human ovarian cancer, MCF-7 breast cancer, and SKUT-1B human uterine sarcoma [17]. Both pyrimidines **14** and **16** exhibited growth inhibitory activity against all three cell lines in the low micromolar concentration range (Table 2). As expected, these potencies are modest in comparison with the corresponding activity as inhibitors of CDK2, for reasons that have yet to be fully established. It is possible that this discrepancy arises as a consequence of poor cellular permeability of the pyrimidines [10], or may reflect the partial redundancy of CDK2 as a driver of tumour cell proliferation, as has been reported previously [18,19].

An attempt to rationalize the activity profile, and to hypothesize a binding mode for the newly-designed analogues, was made through molecular modelling. A conformational search in implicit

Table 2
Growth inhibitory potency of compounds **14**, **16** against selected tumour cell lines.

Compd	GI ₅₀ (μM) ^a		
	A2780	MCF7	Skut-1B
14	1.5 ± 0.6	1.7 ± 0.5	1.5 ± 0.06
16	2.2 ± 0.8	3.5 ± 0.6	2.4 ± 0.06

^a Concentration inhibiting cell growth by 50% of control.

solvent was carried out for all compounds, after which the most stable geometries were subjected to quantum-mechanical (QM) refinement. Subsequently, flexible docking was performed. Firstly, the three-dimensional structure of CDK2 complexed with NU6027 (PDB ID 1E1X) [7] was chosen as the model system. While we were able to reproduce the co-crystallized pose of NU6027 within a root-mean-square (RMS) tolerance of 0.76 Å, we failed to dock the newly synthesized analogue **5**. When **5** was manually superposed on NU6027, a steric clash between the 5-cyanoazoxy group and Lys33 was observed, which prevented its docking. We analysed all crystal structures of CDK2 available in the Protein Data Bank, finding that the side chain of Lys33 is quite flexible and can assume different conformations: in most of the structures this residue does not protrude into the active site as it does in 1E1X. Therefore, the 1E1X structure was replaced by 2C60 [20], because of its good resolution and of the resemblance of the co-crystallised inhibitor NU6102 (**3**, Fig. 1) to our compounds. Again, we were able to reproduce the crystallographic pose of NU6102 inside the binding site within an RMS deviation of 0.30 Å. Additionally, both NU6027 and **5** could be docked in an orientation very similar to that occurring with NU6027 in 1E1X.

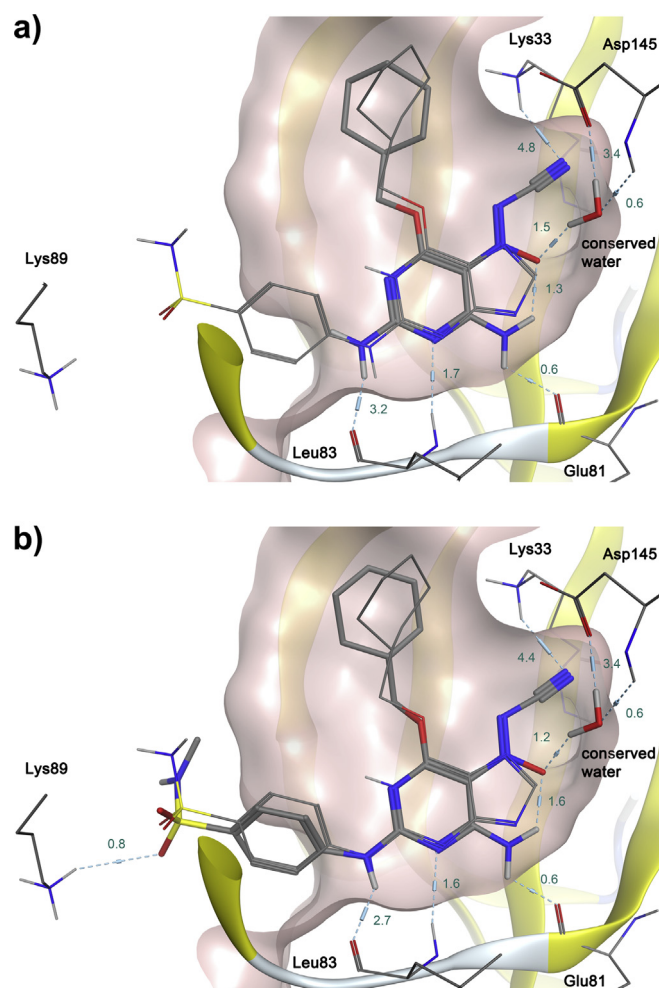


Fig. 4. Binding modes of compounds **5** (a) and **14** (b) (thick sticks) in the active site of CDK2 (PDB structure ID: 2C60); the pose of the co-crystallized inhibitor **3** (thin sticks) is reported for comparison. The binding site is put into evidence through its Connolly surface, while secondary structure elements are represented as flat ribbons (β -sheet segments) and tubes (loops). Hydrogen bonds are depicted with dashed lines; their respective energy magnitudes, as computed by MOE, are reported in kcal mol⁻¹.

Analysing the docking results of **5** against CDK2, the *N*-oxide moiety was found to interact with the side chain carboxyl group of Asp145 via a crystal water molecule, while the cyano group nitrogen establishes a charge-enhanced hydrogen bond with the side chain of Lys33. NU6027 also binds in a similar way, forming a water-mediated hydrogen bond between the nitroso moiety and Asp145 (Fig. 4). As mentioned above, the 5-nitroso group is essential for conferring activity to pyrimidine ligands, enabling, through an intramolecular hydrogen bond, the 6-amino group to establish optimal interactions with Glu81 [7]. To challenge our hypothesis regarding the involvement of a water molecule in binding, we analysed the available crystallographic structures of CDK2 in the Protein Data Bank, and found the water molecule to be highly conserved. When we docked both **5** and NU6027 in the absence of this crystal water, we could not find any pose reminiscent of the crystallographic pose of NU6027. To further corroborate this hypothesis, we built a model of 4-cyclohexylmethoxy-6-aminopyrimidine, namely the NU6027 analogue lacking the 5-nitroso substituent; again, docking was unsuccessful even after constraining the amino group in the same conformation as in NU6027. These findings suggest that the conserved water molecule may significantly contribute to the binding of pyrimidine ligands via an interaction with an appropriate hydrogen bond acceptor at the 5-position. Moreover, the favourable binding affinity of **5** may benefit from the additional, strong hydrogen bonding interaction between the cyano group and the positively charged side chain of Lys33. In the case of compounds **6** and **9**, a small number of productive conformers with low docking scores were found; in particular, the phenylsulfonyl group in **9** is barely compatible with the steric constraints imposed by the size of the cavity. The sulfonamide-substituted derivatives **14** and **16** dock in the active site of CDK2 in an orientation largely superimposable upon NU6102 and **5**, with better docking scores. In addition to the interactions described above, the sulfonamido substituent has an additional hydrogen bonding interaction with the side chain of Lys89, hence the improved affinity against CDK2.

4. Conclusion

In this paper we describe how replacing the nitroso group in the NU6027 lead compound with a cyano-*NNO*-azoxy function resulted in derivatives having potent inhibitory activity against CDKs, with pronounced selectivity for the CDK2 isoform. Substitution of the cyano group with either carbamoyl or phenylsulfonyl moieties failed to improve affinity, while *p*-aminosulfonylphenyl substitution on the 2-NH₂ function proved beneficial, in accordance with established SARs for NU6027. A molecular modelling study showed that compounds **5**, **14** and **16** may adopt a binding mode similar to that determined experimentally for other purine and pyrimidine analogues. This investigation also suggested a significant role for a conserved water molecule in stabilizing the bioactive pose of pyrimidine ligands, through interaction with a suitable hydrogen bond acceptor substituent at the 5-position.

5. Experimental protocols

5.1. Chemistry

Melting points (m.p.) were measured with a capillary apparatus (Büchi 540). M.p. with decomposition were determined after placing the sample in a bath at a temperature 10 °C below the m.p.; a heating rate of 3 °C min⁻¹ was applied. All compounds were routinely checked by FT-IR (Perkin–Elmer SPECTRUM BXII), ¹H and ¹³C NMR (Bruker Avance 300) and mass spectrometry (Finnigan-Mat TSQ-700). The following abbreviations were used for labelling

NMR signals: s (singlet), d (doublet), t (triplet), q (quartet), br (broad), vbr (very broad). Flash column chromatography was performed on silica gel (Merck Kieselgel 60, 230–400 mesh ASTM) using the indicated eluents. Thin layer chromatography (TLC) was carried out on 5 × 20 cm plates with 0.25 mm layer thickness. Anhydrous MgSO₄ was used as drying agent for the organic phases. Analyses (C, H, N) of the new compounds were performed by REDOX (Monza, Italy); the results were within ±0.4% of the theoretical values. Compounds **1** [7], **10** [9], **11** [21], **15** [9] were synthesized following methods described in the literature.

5.1.1. 5-(Cyano-*NNO*-azoxy)-6-(cyclohexylmethoxy)pyrimidine-2,4-diamine (**5**)

To the stirred suspension of **1** (0.502 g, 2 mmol) and cyanamide (0.252 g, 6 mmol) in CH₃CN (25 mL), IBA was added (0.772 g, 2.4 mmol) in portions at r.t. The colour of the reaction mixture changed gradually from purple to yellow. The precipitated yellow solid was filtered off, washed twice with CH₃CN and recrystallized to obtain **2** as a yellow crystalline solid (0.344 g; yield 59%). M.p. 203–204 °C (CH₃CN); ¹H NMR (300 MHz, DMSO-*d*₆) δ 1.14 (m, 5H, C₆H₁₁), 1.77 (m, 6H, C₆H₁₁), 4.13 (d, *J* = 6 Hz, 2H, CH₂O), 7.44 (br s, 1H, NH₂, D₂O exchangeable), 7.50 (br s, 1H, NH₂, D₂O exchangeable), 8.13 (br s, 2H, NH₂, D₂O exchangeable); ¹³C NMR (75 MHz, DMSO-*d*₆) δ 25.1, 25.9, 28.9, 36.4, 72.0, 106.2, 112.3, 159.2, 160.8, 164.2; MS (EI, 70 eV) *m/z* 291 (M⁺), 251 (M–0, 100%), 155, 138. Anal. C₁₂H₁₇N₇O₂ (C, H, N).

5.1.2. 5-(Aminocarbonyl-*NNO*-azoxy)-6-(cyclohexylmethoxy)pyrimidine-2,4-diamine (**6**)

Hydrogen chloride was bubbled during a few minutes into a THF/H₂O (6/1, 30 mL) solution of **5** (0.291 g, 1 mmol) kept at 0 °C. EtOAc (10 mL) and a saturated solution of NaHCO₃ (20 mL) were then added, and the cooled reaction mixture was neutralized with 6 M NaOH under stirring. The aqueous phase was separated and extracted twice with EtOAc. The combined organic phases were dried with brine, then with MgSO₄, and evaporated to give a green oil that was purified by flash chromatography (CH₂Cl₂/MeOH 95/5). The pure yellow solid thus obtained (0.145 g; yield 47%) was recrystallized. M.p. 149–150 °C (MeOH/H₂O); ¹H NMR (300 MHz, DMSO-*d*₆) δ 1.15 (m, 2H, C₆H₁₁), 1.22 (m, 3H, C₆H₁₁), 1.70 (m, 6H, C₆H₁₁), 4.03 (d, *J* = 6 Hz, 2H, CH₂O), 6.60 (br s, 2H, NH₂, D₂O exchangeable), 6.79 (br s, 2H, NH₂, D₂O exchangeable), 7.53 (br s, 1H, NH₂, D₂O exchangeable), 7.63 (br s, 1H, NH₂, D₂O exchangeable); ¹³C NMR (75 MHz, DMSO-*d*₆) δ 25.2, 25.8, 28.8, 36.6, 70.8, 106.3, 157.7, 158.7, 160.7, 162.3; MS (CI, 70 eV) *m/z* 310 (M⁺+1). Anal. C₁₂H₁₉N₇O₃ (C, H, N).

5.1.3. 7-(Cyclohexylmethoxy)-[1,2,5]oxadiazolo[3,4-*d*]pyrimidine-5-amine (**7**)

To the stirred solution of **1** (0.251 g, 1 mmol) and TsNH₂ (0.513 g, 3 mmol) in CH₃CN (12 mL), IBA was added (0.386 g, 1.2 mmol) in portions at r.t. The colour of the reaction mixture gradually changed from purple to grey to green. The precipitate was filtered off, washed twice with CH₃CN and dried to obtain **7** (0.174 g; yield 70%). M.p. 198–199 °C (dec.); ¹H NMR (300 MHz, DMSO-*d*₆) δ 1.20 (m, 5H, C₆H₁₁), 1.71 (m, 6H, C₆H₁₁), 4.38 (d, *J* = 5.7 Hz, 2H, CH₂O), 7.90 (br s, 1H, NH₂, D₂O exchangeable), 7.82 (br s, 1H, NH₂, D₂O exchangeable); ¹³C NMR (75 MHz, DMSO-*d*₆) δ 162.7, 160.4, 135.0, 72.8, 36.2, 28.9, 25.8, 24.7; MS (EI, 70 eV) *m/z* 249 (M⁺), 154 (100%), 97.

5.1.4. *N,N'*-[6-(Cyclohexylmethoxy)-5-nitrosopyrimidine-2,4-diyl]diacetamide (**1a**)

A solution of **1** (0.251 g, 1 mmol) in Ac₂O (3 mL) was stirred at 50 °C for 20 h under dry atmosphere. The solution was then slowly poured into a stirred ice–water mixture; the separated green oil

was triturated to transform it into a green solid, which was then collected on a filter, washed twice with water and dried *in vacuo* on P₂O₅ for 3 days (0.299 g; yield 89%). M.p. 171–172 °C; ¹H NMR (300 MHz, DMSO-*d*₆) δ 1.23 (m, 5H, C₆H₁₁), 1.80 (m, 6H, C₆H₁₁), 2.34 (s, 3H, CH₃), 2.57 (s, 3H, CH₃), 4.47 (d, *J* = 6.6 Hz, 2H, CH₂O), 11.20 (br s, 1H, NH, D₂O exchangeable), 11.53 (br s, 1H, NH, D₂O exchangeable); ¹³C NMR (75 MHz, DMSO-*d*₆) δ 25.5, 26.0, 26.3, 27.5, 29.4, 37.1, 73.5, 139.8, 144.7, 159.7, 169.6, 170.5, 173.1; MS (EI, 70 eV) *m/z* 335 (M⁺), 197 (100%), 155, 84.

5.1.5. *N,N'*-{6-(Cyclohexylmethoxy)-5-[(4-methylphenyl)sulfonyl]-*NNO*-azoxy}pyrimidine-2,4-diyl]diacetamide (**8**) and *N*-[7-(cyclohexylmethoxy)[1,2,5]oxadiazolo[3,4-*d*]pyrimidin-5-yl]acetamide (**7a**)

To the stirred solution of **1a** (0.335 g, 1 mmol) and TsNH₂ (0.342 g, 2 mmol) in CH₂Cl₂/CH₃CN 2/1 (17 mL), IBA (0.644 g, 2 mmol) was added portion-wise at 40 °C. The colour of the reaction mixture gradually changed from purple to orange. After 20 h, when all starting materials had been consumed (TLC), water (10 mL) was added to the reaction mixture, then the aqueous phase was separated and extracted twice with CH₂Cl₂. The combined organic phases were washed with 5% NaHCO₃, brine and dried over MgSO₄. The solvent was removed *in vacuo*, and the resulting crude oil was purified by flash chromatography (petroleum ether/acetone 7/3) to give, eluting first, **7a** (0.079 g; white solid, yield 27%), and, eluting second, the desired product **8** (0.131 g; yellow solid, yield 26%). Compound **7a**: m.p. 290–291 °C; ¹H NMR (300 MHz, CDCl₃) δ 1.25 (m, 5H, C₆H₁₁), 1.86 (m, 6H, C₆H₁₁), 2.72 (s, 3H, CH₃), 4.46 (d, *J* = 6.6 Hz, 2H, CH₂O), 8.04 (br s, 1H, NH, D₂O exchangeable); ¹³C NMR (75 MHz, CDCl₃) δ 25.4, 26.0, 25.9, 26.2, 29.4, 36.8, 75.2, 135.2, 157.3, 161.7, 162.5, 171.8; MS (CI, 70 eV) *m/z* 292 (M⁺+1). Compound **8**: m.p. 170–173 °C (dec.); ¹H NMR (300 MHz, CDCl₃) δ 1.20 (m, 5H, C₆H₁₁), 1.72 (m, 6H, C₆H₁₁), 2.13 (s, 3H, COCH₃), 2.46 (s, 3H, COCH₃), 2.61 (s, 3H, PhCH₃), 4.15 (d, *J* = 6 Hz, 2H, CH₂O), 7.36 (d, *J* = 8.1 Hz, 2H, ArH), 8.01 (d, *J* = 8.4 Hz, 2H, ArH), 9.40 (br s, 1H, NH, D₂O exchangeable), 10.22 (br s, 1H, NH, D₂O exchangeable); ¹³C NMR (75 MHz, CDCl₃) δ 21.8, 23.9, 25.6, 25.9, 26.2, 29.3, 36.9, 74.6, 116.6, 129.4, 130.2, 133.1, 145.6, 153.1, 155.4, 163.9, 168.9, 173.1; MS (CI, 70 eV) *m/z* 505 (M⁺+1), 333 (100%).

5.1.6. 6-Cyclohexylmethoxy-5-[(4-methylphenyl)sulfonyl]-*NNO*-azoxy}pyrimidine-2,4-diamine (**9**)

Compound **7** (0.252 g, 0.5 mmol) was dissolved in EtOH (35 mL) and anhydrous ZnCl₂ (0.239 g, 5 mmol) was added to the solution as a single portion. The mixture was stirred at 65 °C until all starting materials had been consumed (48 h, TLC). The yellow solid formed during the reaction was collected, washed with water, dried and recrystallized (0.123 g; yield 59%). M.p. 227–228 °C (CH₃CN); ¹H NMR (300 MHz, DMSO-*d*₆) δ 0.98 (m, 2H, C₆H₁₁), 1.22 (m, 3H, C₆H₁₁), 1.67 (m, 6H, C₆H₁₁), 2.41 (s, 3H, PhCH₃), 4.04 (d, *J* = 6 Hz, 2H, CH₂O), 7.24 (br s, 2H, NH₂, D₂O exchangeable), 7.44 (d, *J* = 7.8 Hz, 2H, ArH), 7.64 (br s, 2H, NH₂, D₂O exchangeable), 7.83 (d, *J* = 8.1 Hz, 2H, ArH); ¹³C NMR (75 MHz, DMSO-*d*₆) δ 21.0, 25.1, 25.8, 28.8, 36.5, 71.9, 105.8, 128.6, 129.4, 134.9, 144.5, 159.1, 160.7, 164.0; MS (CI, 70 eV) *m/z* 421 (M⁺+1). Anal. C₁₈H₂₄N₆O₄S (C, H, N).

5.1.7. 4-(6-Amino-4-cyclohexylmethoxy)pyrimidin-2-ylamino)-amino-*N*-methylbenzenesulfonamide trifluoroacetate salt (**12**)

To a solution of **10** (2.640 g, 8 mmol) and **11** (1.500 g, 8 mmol) in TFE (35 mL), TFA (3.10 mL, 40 mmol) was added. The resulting mixture was stirred for 10 min at r.t., then refluxed for 24 h at 80 °C. The precipitated solid was collected on a filter and washed with EtOAc to afford **12** as a white crystalline solid (1.500 g). Solvents were removed *in vacuo* from the filtrate, water (30 mL) was added, the pH was adjusted to neutral with saturated aqueous NaHCO₃ and

the mixture was extracted with EtOAc. The combined organic layers were washed with H₂O, followed by brine, dried over MgSO₄, and the solvent was removed *in vacuo*. The crude oil was purified by flash chromatography (CH₂Cl₂/MeOH 9.7/0.3) to obtain an additional crop of **12** as the free base (0.700 g; overall yield 59%). M.p. 210–212 °C (MeOH); ¹H NMR (300 MHz, DMSO-*d*₆) δ 0.99–1.26 (m, 5H, C₆H₁₁), 1.69–1.77 (m, 6H, C₆H₁₁), 2.39 (s, 3H, CH₃), 4.03 (d, *J* = 6 Hz, 2H, CH₂O), 5.35 (s, 1H, H₅), 6.90 (vbr s, 2H, NH₂, D₂O exchangeable), 7.23 (br s, 2H, NH₂, D₂O exchangeable), 7.63 (d, *J* = 8.7 Hz, 2H, ArH), 7.93 (d, *J* = 9.0 Hz, 2H, ArH), 9.67 (s, 1H, NH, D₂O exchangeable); ¹³C NMR (75 MHz, DMSO-*d*₆) δ 169.4, 163.9 br, 156.5 br, 143.8 br, 130.9 br, 127.5, 118.5 br, 78.4, 71.0, 36.7, 29.1, 28.6, 25.9, 25.1; MS (EI, 70 eV) *m/z* 391 (M⁺), 361, 295 (100%). Anal. C₁₈H₂₅N₅O₃S·CF₃COOH (C, H, N).

5.1.8. 4-(6-Amino-5-nitroso-4-cyclohexylmethoxy)pyrimidin-2-ylamino)-amino-*N*-methylbenzenesulfonamide (**13**)

A suspension of **12** (1.173 g, 3 mmol) in glacial acetic acid (20 mL) was solubilized at 95 °C, then a solution of NaNO₂ (0.276 g, 4 mmol) in water (3 mL) was added drop-wise while the colour of the reaction mixture slowly changed to green. The reaction mixture was stirred at 95 °C for 1 h, then treated with EtOAc (100 mL). The organic phase was washed with H₂O, 5% NaHCO₃, H₂O, brine, and dried over MgSO₄. The solvent was evaporated and the resulting crude oil was purified by flash chromatography (CH₂Cl₂/iPrOH 9.6/0.4) to afford **13** as a green crystalline solid (0.580 g; yield 46%). M.p. 157–158 °C (MeOH); ¹H NMR (300 MHz, DMSO-*d*₆) δ 1.05–1.30 (m, 5H, C₆H₁₁), 1.70–1.83 (m, 6H, C₆H₁₁), 2.40 (d, *J* = 5.1 Hz, 3H, NHCH₃), 4.43 (d, *J* = 6.3 Hz, 2H, CH₂O), 7.37 (q, *J* = 5.1 Hz, 1H, NHCH₃, D₂O exchangeable), 7.71 (d, *J* = 8.4 Hz, 2H, ArH), 8.11 (br s, 2H, ArH), 8.61 (vbr s, 1H, 6-NH₂, D₂O exchangeable), 10.19 (vbr s, 1H, 6-NH₂, D₂O exchangeable), 10.57 (s, 1H, NH, D₂O exchangeable); ¹³C NMR (75 MHz, DMSO-*d*₆) δ 26.0, 26.8, 29.5, 30.0, 37.6, 73.1 br, 121.3 br, 128.3, 134.0, 141.0, 143.4, 150.1 br, 160.4 br, 171 vbr; MS (EI, 70 eV) *m/z* 420 (M⁺), 324 (100%). Anal. C₁₈H₂₄N₆O₄S·0.5H₂O (C, H, N).

5.1.9. 4-[6-Amino-5-(cyano-*NNO*-azoxy)-4-cyclohexylmethoxy]pyrimidin-2-ylamino)-amino-*N*-methylbenzenesulfonamide (**14**)

To a stirred suspension of **13** (0.270 g, 0.643 mmol) and cyanamide (0.084 g, 2.0 mmol, 3.0 equiv) in CH₃CN (3.0 mL), IBA (0.350 g, 1.28 mmol, 2.0 equiv) was added portion-wise at r.t. After 2 h the reaction mixture was extracted with CH₂Cl₂ (100 mL), washed with H₂O (2 × 30 mL) and brine, dried (MgSO₄) and evaporated to dryness. The resulting crude product was purified by flash chromatography (CH₂Cl₂/MeOH 9.5/0.5), then recrystallized from iPrOH to afford **14** as a yellow crystalline solid (0.100 g; yield 34%). M.p. 140–143 °C (dec.); ¹H NMR (300 MHz, DMSO-*d*₆) δ 1.09–1.24 (m, 5H, C₆H₁₁), 1.60–1.81 (m, 6H, C₆H₁₁), 2.40 (d, *J* = 4.8 Hz, 3H, NHCH₃), 4.24 (d, *J* = 5.4 Hz, 2H, CH₂O), 7.35 (br q, 1H, NHCH₃, D₂O exchangeable), 7.68 (d, *J* = 8.4 Hz, 2H, ArH), 8.06 (br s, 2H, ArH), 8.40 (vbr s, 2H, 6-NH₂, D₂O exchangeable), 10.32 (s, 1H, NH, D₂O exchangeable); ¹³C NMR (75 MHz, DMSO-*d*₆) δ 25.1, 25.8, 28.5, 28.8, 36.4, 72.7, 107.2, 111.8, 119.7, 127.3, 132.4, 142.7, 156.9, 158.7, 163.9; MS (EI, 70 eV) *m/z* 460 (M⁺), 420, 324 (100%). Anal. C₁₉H₂₄N₈O₄S·0.25H₂O·0.25iPrOH (C, H, N).

5.1.10. 4-[6-Amino-5-(cyano-*NNO*-azoxy)-4-cyclohexylmethoxy]pyrimidin-2-ylamino)-amino-*N*-(2-hydroxyethyl)-benzenesulfonamide (**16**)

To a stirred suspension of **15** (0.150 g, 0.333 mmol) and cyanamide (0.042 g, 0.99 mmol, 3.0 equiv) in CH₃CN (3.0 mL), IBA (0.021 g, 6.7 mmol, 2.0 equiv) was added portion-wise at r.t. After 2 h the reaction mixture was heated to 35 °C for 30 min, then extracted with CH₂Cl₂ (100 mL), washed with H₂O (2 × 30 mL) and brine, dried

(MgSO₄) and evaporated to dryness. The resulting crude product was purified by flash chromatography (CH₂Cl₂/MeOH 9.5/0.5), then recrystallized from methanol to yield **16** as a yellow crystalline solid (0.140 g; yield 86%). M.p. 209–211 °C (MeOH); ¹H NMR (300 MHz, DMSO-*d*₆) δ 1.03–1.26 (m, 5H, C₆H₁₁), 1.65–1.78 (m, 6H, C₆H₁₁), 2.78 (q, *J* = 12.0 Hz, 2H, NHCH₂), 3.36 (m, 2H, HOCH₂), 4.24 (d, *J* = 6 Hz, 2H, CH₂O), 4.68 (t, *J* = 5.4 Hz, 1H, OH, D₂O exchangeable), 7.49 (t, 1H, NH, D₂O exchangeable), 7.69 (d, *J* = 8.7 Hz, 2H, ArH), 8.04 (br d, *J* = 7.5 Hz, 2H, ArH), 8.40 (vbr s, 2H, NH₂, D₂O exchangeable), 10.31 (s, 1H, NH, D₂O exchangeable); ¹³C NMR (75 MHz, DMSO-*d*₆) δ 25.6, 26.4, 29.4, 37.0, 45.5, 60.3, 73.3, 107.5, 112.0, 120.2, 127.7, 134.0, 142.9, 157.2, 158.9, 164.2; MS (EI, 70 eV) *m/z* 490 (M⁺), 450, 354 (100%). Anal. C₂₀H₂₆N₈O₅S · 0.5H₂O (C, H, N).

5.2. Molecular modelling

The molecular models of the newly synthesized analogues were generated using standard bond lengths and angles with MOE [22]. Energy minimization was carried out with the MMFF94s force field (MMFF94 charges, Generalized Born implicit solvent model) using a truncated Newton–Raphson geometry optimization method, until the gradient was below 0.001 kcal mol⁻¹. The conformational space of the models was explored by means of a stochastic conformational search, as implemented in MOE. Further optimization of the global minimum geometry was achieved by *ab initio* quantum-mechanical (QM) calculations at the UHF/6-31G(d) level of theory using GAMESS-US [23]. Electrostatic charges were fitted on the QM electrostatic potential through the RESP method [24] as implemented in AMBER 10 [25]. Crystal structures of human CDK2 complexes with different ligands were retrieved from the Protein Data Bank. Sections with missing residues (namely, residues 36–43 in 1E1X and residues 38–43, 297, 298 in 2C6O) were not modelled, since they were far from the active site; instead, the C and N-terminals at the ends of the missing section were capped with N-methylamide and acetyl groups, respectively. Hydrogen atoms were added to the protein–ligand complex in standard positions, and then minimized through the SANDER module of the AMBER 10 suite, while keeping heavy atoms restrained to their original positions by a harmonic potential (10³ kcal mol⁻¹ Å⁻²). All molecular mechanics calculations on the protein–ligand complexes were carried out using FF99SB and GAFF parameters for protein and ligand, respectively. After removing the co-crystallized ligand, docking simulations were performed using AutoDock 4.2 [26]. A grid with 0.375 Å step size encompassing the whole active site was generated with AutoGrid, then 100 flexible docking runs were carried out with AutoDock, using the Lamarckian genetic algorithm with default parameters.

Acknowledgements

The Chemical Computing Group is acknowledged for financial support to computational work.

Appendix A. Supplementary data

Supplementary data associated with this article can be found in the online version, at <http://dx.doi.org/10.1016/j.ejmech.2013.07.031>.

References

- [1] V. Mesguiche, R.J. Parsons, C.E. Arris, J. Bentley, F.T. Boyle, N.J. Curtin, T.G. Davies, J.A. Endicott, A.E. Gibson, B.T. Golding, R.J. Griffin, P. Jewsbury, L.N. Johnson, D.R. Newell, M.E.M. Noble, L.Z. Wang, I.R. Hardcastle, 4-Alkoxy-2,6-diaminopyrimidine derivatives: inhibitors of cyclin dependent kinases 1 and 2, *Bioorg. Med. Chem. Lett.* 13 (2003) 217–222.
- [2] M. Malumbres, M. Barbacid, Mammalian cyclin-dependent kinases, *Trends Biochem. Sci.* 30 (2005) 630–641.
- [3] M. Malumbres, M. Barbacid, Cell cycle, CDKs and cancer: a changing paradigm, *Nat. Rev. Cancer* 9 (2009) 153–166.
- [4] S. Lapenna, A. Giordano, Cell cycle kinases as therapeutic targets for cancer, *Nat. Rev. Drug Discovery* 8 (2009) 547–566.
- [5] J. Ciceinas, M. Valius, The CDK inhibitors in cancer research and therapy, *J. Cancer Res. Clin. Oncol.* 137 (2011) 1409–1418.
- [6] M. Guha, Blockbuster dreams for Pfizer's CDK inhibitor, *Nat. Biotechnol.* 31 (2013) 187.
- [7] C.E. Arris, F.T. Boyle, A.H. Calvert, N.J. Curtin, J.A. Endicott, E.F. Garman, A.E. Gibson, B.T. Golding, S. Grant, R.J. Griffin, P. Jewsbury, L.N. Johnson, A.M. Lawrie, D.R. Newell, M.E.M. Noble, E.A. Sausville, R. Schultz, W. Yu, Identification of novel purine and pyrimidine cyclin-dependent kinase inhibitors with distinct molecular interactions and tumor cell growth inhibition profiles, *J. Med. Chem.* 43 (2000) 2797–2804.
- [8] I.R. Hardcastle, C.E. Arris, J. Bentley, F.T. Boyle, Y.H. Chen, N.J. Curtin, J.A. Endicott, A.E. Gibson, B.T. Golding, R.J. Griffin, P. Jewsbury, J. Menyerol, V. Mesguiche, D.R. Newell, M.E.M. Noble, D.J. Pratt, L.Z. Wang, H.J. Whitfield, N-2-Substituted O-6-cyclohexylmethylguanidine derivatives: potent inhibitors of cyclin-dependent kinases 1 and 2, *J. Med. Chem.* 47 (2004) 3710–3722.
- [9] F. Marchetti, K.L. Sayle, J. Bentley, W. Clegg, N.J. Curtin, J.A. Endicott, B.T. Golding, R.J. Griffin, K. Haggerty, R.W. Harrington, V. Mesguiche, D.R. Newell, M.E.M. Noble, R.J. Parsons, D.J. Pratt, L.Z. Wang, I.R. Hardcastle, Structure-based design of 2-aryl amino-4-cyclohexylmethoxy-5-nitroso-6-aminopyrimidine inhibitors of cyclin-dependent kinase 2, *Org. Biomol. Chem.* 5 (2007) 1577–1585.
- [10] F. Marchetti, C. Cano, N.J. Curtin, B.T. Golding, R.J. Griffin, K. Haggerty, D.R. Newell, R.J. Parsons, S.L. Payne, L.Z. Wang, I.R. Hardcastle, Synthesis and biological evaluation of 5-substituted O⁴-alkylpyrimidines as CDK2 inhibitors, *Org. Biomol. Chem.* 8 (2010) 2397–2407.
- [11] A. Gasco, A. Serafino, V. Mortarini, E. Menziani, M.A. Bianco, J. Ceruti Scurti, An antibacterial and antifungal compound from *Calvatia lilacina*, *Tetrahedron Lett.* 15 (1974) 3431–3432.
- [12] H. Umezawa, T. Takeuchi, H. Linuma, M. Ito, M. Ishizuka, Y. Kurakata, Y. Umeda, Y. Nakanishi, T. Nakamura, A. Obayashi, O. Tanabe, A new antibiotic, calvatic acid, *J. Antibiot.* 28 (1975) 87–90.
- [13] T. Okuda, N. Nakayama, A. Fujiwara, Calvatic acid production by *Lycoperdon perniceum*, *Trans. Mycol. Soc. Jpn.* 23 (1982) 225–234.
- [14] R. Fruttero, G. Mulatero, R. Calvino, A. Gasco, A directed synthesis of alkyl, aryl, and heteroaryl-ONN-azoxycyanides, *J. Chem. Soc., Chem. Commun.* 5 (1984) 323–324.
- [15] M. Sako, S. Oda, K. Hirota, G.P. Beardsley, Convenient and versatile synthetic methods for furazano[3,4-*d*]pyrimidines, *Synthesis* 11 (1997) 1255–1257.
- [16] D.L. Lipilin, A.M. Churakov, S.L. Ioffe, Y.A. Strelenko, V.A. Tartakovskiy, Nucleophilic aromatic substitution of hydrogen in the reaction of *tert*-alkylamines with nitrosobenzenes – synthesis and NMR study of *N*-(*tert*-alkyl)-*ortho*-nitrosoanilines, *Eur. J. Org. Chem.* 1 (1999) 29–35.
- [17] M. Pennati, A.J. Campbell, M. Curto, M. Binda, Y. Cheng, L.-Z. Wang, N.J. Curtin, B.T. Golding, R.J. Griffin, I.R. Hardcastle, A. Henderson, N. Zaffaroni, D.R. Newell, Potentiation of paclitaxel-induced apoptosis by the novel cyclin-dependent kinase inhibitor NU6140: a possible role for survivin down-regulation, *Mol. Cancer Ther.* 4 (2005) 1328–1337.
- [18] O. Tetsu, F. McCormick, Proliferation of cancer cells despite CDK2 inhibition, *Cancer Cell* 3 (2003) 233–245.
- [19] S. Ortega, I. Presto, J. Odajima, A. Martín, P. Dubus, R. Sotillo, J.L. Barbero, M. Malumbres, M. Barbacid, Cyclin-dependent kinase 2 is essential for meiotic but not for mitotic cell division in mice, *Nat. Genet.* 35 (2003) 25–31.
- [20] C.M. Richardson, D.S. Williamson, M.J. Parratt, J. Borgognoni, A.D. Cansfield, P. Dokurno, G.L. Francis, R. Howes, J.D. Moore, J.B. Murray, A. Robertson, A.E. Surgenor, C.J. Torrance, Triazolo[1,5-*a*]pyrimidines as novel CDK2 inhibitors: protein structure-guided design and SAR, *Bioorg. Med. Chem. Lett.* 16 (2006) 1353–1357.
- [21] I.K. Khanna, R.M. Weier, Y. Yu, P.W. Collins, J.M. Miyashiro, C.M. Koboldt, A.W. Veenhuizen, J.L. Currie, K. Seibert, P.C. Isakson, 1,2-Diarylpyrroles as potent and selective inhibitors of cyclooxygenase-2, *J. Med. Chem.* 40 (1997) 1619–1633.
- [22] MOE Version 2010.11, Chemical Computing Group Inc., Montreal, Quebec, Canada, 2011.
- [23] M.W. Schmidt, K.K. Baldridge, J.A. Boatz, S.T. Elbert, M.S. Gordon, J.H. Jensen, S. Koseki, N. Matsunaga, K.A. Nguyen, S.J. Su, T.L. Windus, M. Dupuis, J.A. Montgomery, General atomic and molecular electronic structure system, *J. Comput. Chem.* 14 (1993) 1347–1363.
- [24] J. Wang, P. Cieplak, P.A. Kollman, How well does a restrained electrostatic potential (RESP) model perform in calculating conformational energies of organic and biological molecules? *J. Comput. Chem.* 21 (2000) 1049–1074.
- [25] D.A. Case, T.A. Darden, T.E. Cheatham III, C.L. Simmerling, J. Wang, R.E. Duke, R. Luo, M. Crowley, R.C. Walker, W. Zhang, K.M. Merz, B. Wang, S. Hayik, A. Roitberg, G. Seabra, I. Kolossvary, K.F. Wong, F. Paesani, J. Vanicek, X. Wu, S.R. Brozell, T. Steinbrecher, H. Gohlke, L. Yang, C. Tan, J. Mongan, V. Hornak, G. Cui, D.H. Mathews, M.G. Seetin, C. Sagui, V. Babin, P.A. Kollman, AMBER 10, University of California, San Francisco, USA, 2008.
- [26] G.M. Morris, R. Huey, W. Lindstrom, M.F. Sanner, R.K. Belew, D.S. Goodsell, A.J. Olson, Autodock4 and AutoDockTools4: automated docking with selective receptor flexibility, *J. Comput. Chem.* 16 (2009) 2785–2791.